

REPORT DOCUMENTATION PAGE				Form Approved OMB NO. 0704-0188	
<p>The public reporting burden for this collection of information is estimated to average 1 hour per response, including the time for reviewing instructions, searching existing data sources, gathering and maintaining the data needed, and completing and reviewing the collection of information. Send comments regarding this burden estimate or any other aspect of this collection of information, including suggestions for reducing this burden, to Washington Headquarters Services, Directorate for Information Operations and Reports, 1215 Jefferson Davis Highway, Suite 1204, Arlington VA, 22202-4302. Respondents should be aware that notwithstanding any other provision of law, no person shall be subject to any penalty for failing to comply with a collection of information if it does not display a currently valid OMB control number.</p> <p>PLEASE DO NOT RETURN YOUR FORM TO THE ABOVE ADDRESS.</p>					
1. REPORT DATE (DD-MM-YYYY)		2. REPORT TYPE New Reprint		3. DATES COVERED (From - To) -	
4. TITLE AND SUBTITLE Lasing and longitudinal cavity modes in photo-pumped deep ultraviolet AlGa _N heterostructures				5a. CONTRACT NUMBER	
				5b. GRANT NUMBER W911NF-04-D-0003	
				5c. PROGRAM ELEMENT NUMBER 611102	
6. AUTHORS Jinqiao Xie, Seiji Mita, Zachary Bryan, Wei Guo, Lindsay Hussey, Baxter Moody, Raoul Schlessler, Ronny Kirste, Michael Gerhold, Ramon Collazo, Zlatko Sitar				5d. PROJECT NUMBER	
				5e. TASK NUMBER	
				5f. WORK UNIT NUMBER	
7. PERFORMING ORGANIZATION NAMES AND ADDRESSES North Carolina State University Research Administration 2701 Sullivan Drive, Suite 240 Raleigh, NC 27695 -7514				8. PERFORMING ORGANIZATION REPORT NUMBER	
9. SPONSORING/MONITORING AGENCY NAME(S) AND ADDRESS(ES) U.S. Army Research Office P.O. Box 12211 Research Triangle Park, NC 27709-2211				10. SPONSOR/MONITOR'S ACRONYM(S) ARO	
				11. SPONSOR/MONITOR'S REPORT NUMBER(S) 57365-EL-SR.1	
12. DISTRIBUTION AVAILABILITY STATEMENT Approved for public release; distribution is unlimited.					
13. SUPPLEMENTARY NOTES The views, opinions and/or findings contained in this report are those of the author(s) and should not be construed as an official Department of the Army position, policy or decision, unless so designated by other documentation.					
14. ABSTRACT To unambiguously distinguish lasing from super luminescence, key elements of lasing such as longitudinal cavity modes with narrow line-width, polarized emission, and elliptically shaped far-field pattern, need to be demonstrated at the same time. Here, we show transverse electric polarized lasing at 280.8 nm and 263.9 nm for AlGa _N based multi-quantum-wells and double heterojunction structures fabricated on single crystalline AlN substrates. An elliptically shaped					
15. SUBJECT TERMS AlGa _N lasers, optical pumping, longitudinal cavity modes					
16. SECURITY CLASSIFICATION OF:			17. LIMITATION OF ABSTRACT UU	15. NUMBER OF PAGES	19a. NAME OF RESPONSIBLE PERSON Michael Gerhold
a. REPORT UU	b. ABSTRACT UU	c. THIS PAGE UU			19b. TELEPHONE NUMBER 919-549-4357

Report Title

Lasing and longitudinal cavity modes in photo-pumped deep ultraviolet AlGaIn heterostructures

ABSTRACT

To unambiguously distinguish lasing from super luminescence, key elements of lasing such as longitudinal cavity modes with narrow line-width, polarized emission, and elliptically shaped far-field pattern, need to be demonstrated at the same time. Here, we show transverse electric polarized lasing at 280.8 nm and 263.9 nm for AlGaIn based multi-quantum-wells and double heterojunction structures fabricated on single crystalline AlN substrates. An elliptically shaped far-field pattern was recorded when pumped above threshold. With cavities shorter than 200 nm, well-defined, equally spaced longitudinal modes with line widths as narrow as 0.014 nm were observed. The low threshold pumping density of 84kW/cm² suggests that the electrically pumped sub-300 nm ultraviolet laser diodes are imminent. VC 2013 AIP Publishing LLC.

REPORT DOCUMENTATION PAGE (SF298)
(Continuation Sheet)

Continuation for Block 13

ARO Report Number 57365.1-EL-SR
Lasing and longitudinal cavity modes in photo-pu ...

Block 13: Supplementary Note

© 2013 . Published in Appl. Phys. Lett., Vol. Ed. 0 102, (1) (2013), (, (1). DoD Components reserve a royalty-free, nonexclusive and irrevocable right to reproduce, publish, or otherwise use the work for Federal purposes, and to authroize others to do so (DODGARS §32.36). The views, opinions and/or findings contained in this report are those of the author(s) and should not be construed as an official Department of the Army position, policy or decision, unless so designated by other documentation.

Approved for public release; distribution is unlimited.

Lasing and longitudinal cavity modes in photo-pumped deep ultraviolet AlGaIn heterostructures

Jinqiao Xie,^{1(a)} Seiji Mita,¹ Zachary Bryan,² Wei Guo,² Lindsay Hussey,² Baxter Moody,¹ Raoul Schlessler,¹ Ronny Kirste,² Michael Gerhold,³ Ramón Collazo,² and Zlatko Sitar²

¹HexaTech, Inc., 991 Aviation Pkwy., Suite 800, Morrisville, North Carolina 27560, USA

²Department of Materials Science and Engineering, North Carolina State University, Raleigh, North Carolina 27695, USA

³Engineering Science Directorate, Army Research Office, P.O. Box 12211, Research Triangle Park, North Carolina 27703, USA

(Received 27 March 2013; accepted 18 April 2013; published online 29 April 2013)

To unambiguously distinguish lasing from super luminescence, key elements of lasing such as longitudinal cavity modes with narrow line-width, polarized emission, and elliptically shaped far-field pattern, need to be demonstrated at the same time. Here, we show transverse electric polarized lasing at 280.8 nm and 263.9 nm for AlGaIn based multi-quantum-wells and double heterojunction structures fabricated on single crystalline AlN substrates. An elliptically shaped far-field pattern was recorded when pumped above threshold. With cavities shorter than 200 μm , well-defined, equally spaced longitudinal modes with line widths as narrow as 0.014 nm were observed. The low threshold pumping density of 84 kW/cm² suggests that the electrically pumped sub-300 nm ultraviolet laser diodes are imminent. © 2013 AIP Publishing LLC.

[<http://dx.doi.org/10.1063/1.4803689>]

During the last two decades, AlInGaIn-based light emitting diode (LED) and laser diode (LD) technology has rapidly advanced, becoming a cornerstone in a variety of applications ranging from lighting, communications, and spectroscopy to data storage and processing.¹ Despite the progress in deep ultraviolet (UV) LEDs,^{2,3} research on deep UV LDs is very limited.⁴ This is mainly due to technical and scientific barriers arising from the lack of proper crystalline substrates and the poor understanding of defect control in wide bandgap semiconductors that limits the internal quantum efficiency (IQE) of devices. Because of strong carrier localization, InGaIn based multiple quantum well (MQW) structures exhibit a relatively high quantum efficiency even with threading dislocation densities (TDDs) of $1 \times 10^{10} \text{ cm}^{-2}$.⁵ In contrast, optical and electronic properties of AlGaIn and its MQW structures deteriorate rapidly at high TDDs,⁶ which is typical of conventional III-V compound semiconductors.^{7,8} Since threading dislocations can act as current leakage paths, lateral epitaxial overgrowth techniques or bulk GaIn substrates with low TDDs are desired for fabrication of InGaIn-based LDs with long lifetimes.⁹ In contrast, heteroepitaxial AlN layers grown by metal organic chemical vapor deposition (MOCVD) exhibit high TDDs even with sophisticated growth techniques intended to reduce dislocations.¹⁰ Recently, large-area single crystal AlN substrates with TDDs of $\sim 10^3 \text{ cm}^{-2}$ have become available.^{11,12} Using these substrates, homoepitaxial AlN layers grown by MOCVD exhibited excellent optical quality and enabled resolution of a well-defined band edge with fine excitonic structure.¹³ In addition, AlGaIn and AlGaIn heterostructures with uniform Al incorporation were reproducibly grown on these substrates.

For the development of deep UV LDs, it is important to distinguish between superluminescence and lasing in the LD

structure. Superluminescence is spontaneous emission amplified by stimulated emission in the gain medium, and can have an abrupt threshold, much like the onset of lasing.^{14,15} To unambiguously distinguish lasing from superluminescence, several key characteristics of lasing need to be simultaneously demonstrated. These characteristics are: longitudinal modes with narrow line width, polarized emission, and an elliptically shaped far-field pattern. In 2004, Takano reported on a threshold of 1.2 MW/cm² at 241.5 nm for an optically pumped AlGaIn MQW structure grown on a SiC substrate.¹⁶ More recently, a threshold of 126 kW/cm² at 267 nm with transverse electric (TE) polarization was reported for LD structures grown on single crystalline AlN substrates.¹⁷ However, the line width of the reported emission spectra was estimated to be wider than 1 nm, which is relatively broad considering the reported cavity lengths. Moreover, the far-field pattern and longitudinal modes with narrow line width were not observed. In this letter, we report on the observation of well-defined longitudinal TE modes having a full-width-at-half-maximum (FWHM) narrower than 0.02 nm. Above the lasing threshold, an elliptically shaped far-field pattern was clearly recorded. The lasing threshold was 84 kW/cm², which makes it suitable for the fabrication of an injection-pumped laser diode.

Two types of AlGaIn-based structures, MQWs and a double heterojunction (DH), grown on single-crystal *c*-plane AlN substrates were used for this study. MQW structures contained ten pairs of Al_{0.5}Ga_{0.5}N/Al_{0.7}Ga_{0.3}N (1.6 nm well/4 nm barrier) with a 500 nm Al_{0.7}Ga_{0.3}N cladding layer. DH structures had the same cladding layer with a 20 nm thick Al_{0.6}Ga_{0.4}N active region capped by 10 nm of Al_{0.7}Ga_{0.3}N. None of the structures were intentionally doped. The AlGaIn composition was determined by triple-axis high-resolution X-ray diffraction measurements. Cross sectional scanning transmission electron microscopy (STEM) was performed on

^{a)}E-mail: axie@hexatechinc.com

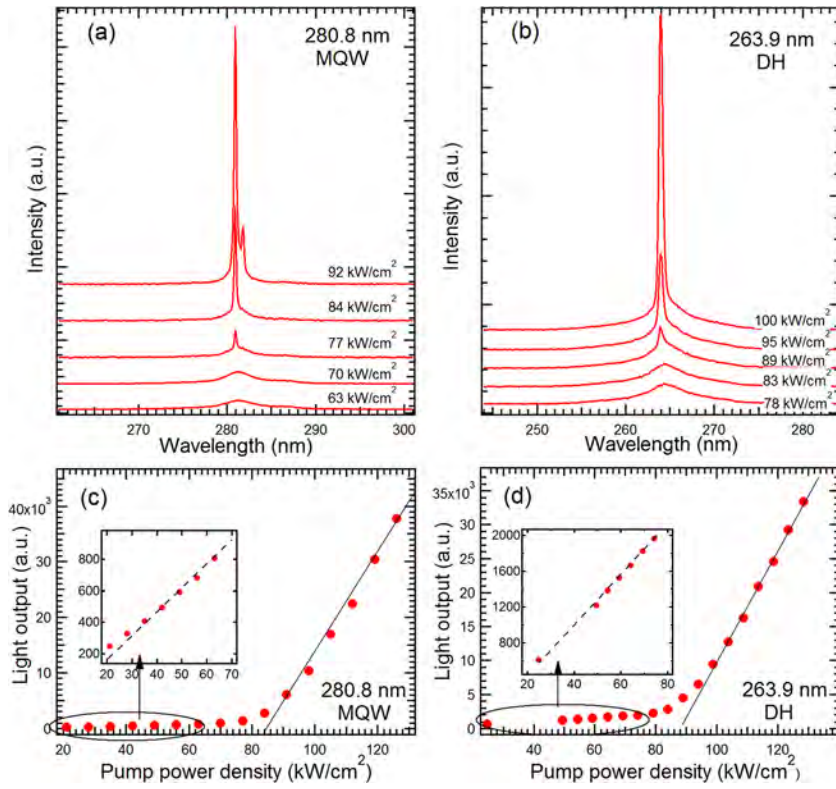


FIG. 1. Room temperature, low-resolution lasing spectra for (a) MQW and (b) DH structures pumped below and above the threshold. The corresponding integrated light output as a function of pumping power density for (c) MQWs and (d) DH, respectively. Cavity length ~ 1.5 mm. Spectra are shifted vertically for clarity.

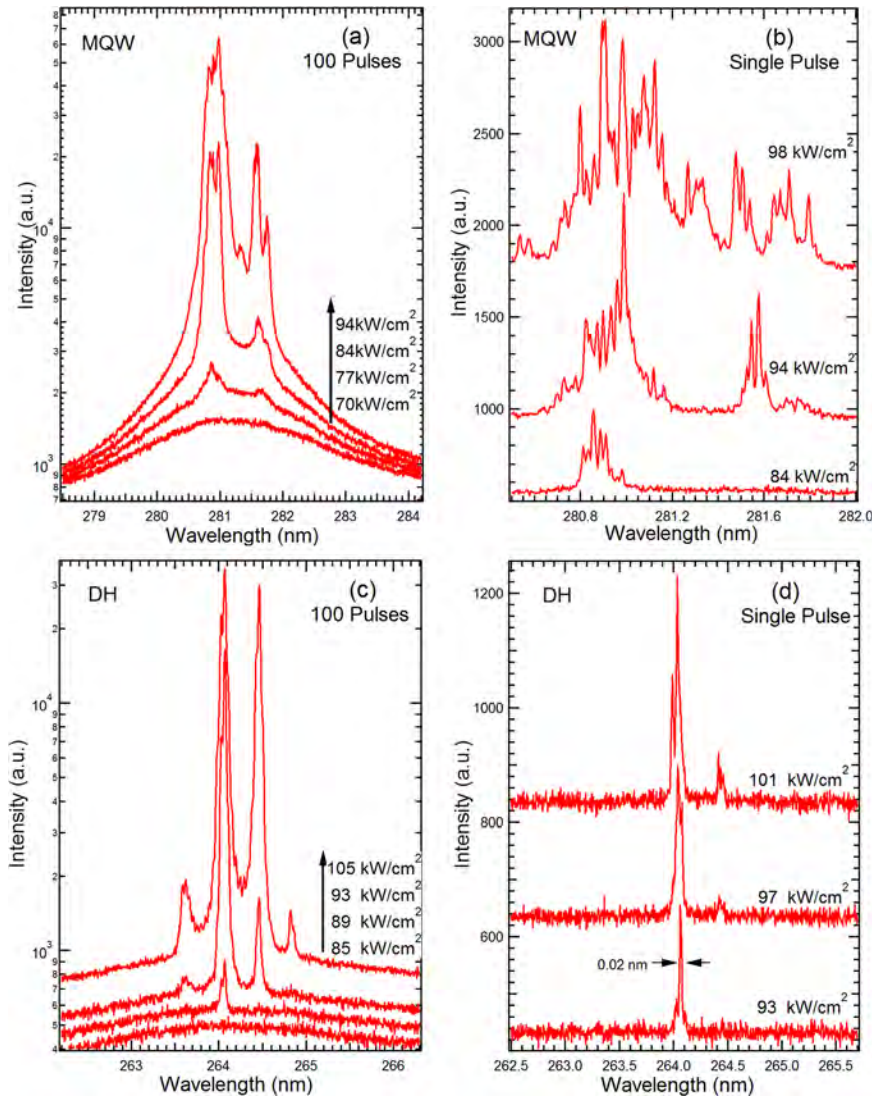


FIG. 2. Room temperature high-resolution lasing spectra for (a) and (b) MQW, (c) and (d) DH pumped below and above the threshold. The spectra were recorded by integrating over (a) and (c) 100 pumping pulses, and (b) and (d) single pumping pulse. Cavity length: ~ 1.5 mm. Spectra are shifted vertically for clarity.

the MQW structure to study the abruptness of the interfaces and the compositional uniformity of individual layers. We did not observe any Al clustering or compositional fluctuations as reported previously.¹⁸ Details on AlN substrate preparation and MOCVD growth process can be found elsewhere.¹⁹ Laser cavities were obtained by cleaving along the *m*-facet of the AlN wafer. For the 1.5 mm long cavity, the cleaving was done with full wafer thickness of 550 μm . To obtain $\sim 200\ \mu\text{m}$ long cavities, wafers were mechanically thinned down to $\sim 150\ \mu\text{m}$ from the backside with an optical finish. A Coherent 193 nm ArF excimer laser with a 5 ns pulse was used as the pumping source and was focused through a cylindrical lens onto the laser bar. Lasing in the structures was realized in an edge-emission configuration. Spectra were collected with a Princeton Instruments Acton SP2750 0.75 m high-resolution spectrograph with three gratings and a PIXIS: 2KBV cooled charge-coupled device camera. For wavelengths from 250 nm to 290 nm, the spectral resolution was 0.1 nm for the 150 grooves/mm grating and 0.004 nm for the 3600 grooves/mm grating. Alpha-BBO Glan-Laser Polarizers from Thorlabs were used for the polarization dependent spectral measurement.

Figures 1(a) and 1(b) show the room temperature low-resolution PL spectra for the two structures. The light output was plotted as a function of pumping power density in Figures 1(c) and 1(d). For low pumping power density (P_{pump}), the PL spectra were dominated by broad spontaneous emission peaks with intensities linearly proportional to the pumping power density [see inset in Figs. 1(c) and 1(d)]. The FWHM of the spontaneous emission peaks was $\sim 4.6\ \text{nm}$ at 281.6 nm and $\sim 6.5\ \text{nm}$ at 264.4 nm, respectively. With increasing pumping power density, sharp peaks started to emerge in both structures and their intensities increased superlinearly. A clear threshold (P_{th}) was observed at $\sim 84\ \text{kW/cm}^2$ for the MQW structure and $\sim 90\ \text{kW/cm}^2$ for the DH structure, respectively. At threshold ($P_{\text{pump}} \sim 84\ \text{kW/cm}^2$), the MQW structure had a peak centered at 280.8 nm with a FWHM of 0.3 nm. When the pumping power density was further increased, the 280.8 nm peak became slightly broader, and a second peak at 281.8 nm appeared. The reason for this behavior was the excitation of additional longitudinal modes at a higher pumping density, as evidenced in the high-resolution spectra. As shown in Figures 1(b) and 1(d), the DH structure followed a similar trend. Above the lasing threshold, both structures showed slope efficiency comparable to that of InGaN-based lasers.²⁰

Figure 2 shows the high-resolution lasing spectra with different integration times for the two structures. Due to the lack of proper laser sources in the deep UV spectral range, excimer lasers are widely used as excitation sources for many optical measurements. However, excimer lasers have poor beam quality and stability. In order to properly measure the threshold power density shown in Figure 1, long integration times (10 s or more) were needed. For this reason, spectra integrated over 100 pulses [Figures 2(a) and 2(c)] showed several peaks and longitudinal cavity modes could not be clearly resolved. In contrast, when the spectra were recorded during a single pump-pulse, as shown in Figures 2(b) and 2(d), many narrow peaks with spacing varying from 0.011 to 0.046 nm were observed. The line width of these narrow

peaks was approximately 0.02 nm. Both measurements are consistent with the onset of the longitudinal cavity modes.

In a laser cavity, longitudinal modes are equally spaced. If the cavity length is d , for a given wavelength (λ) the distance between two neighboring longitudinal modes and the FWHM of an individual mode, $\delta\lambda$, are expressed as²¹

$$\Delta\lambda \sim \frac{\lambda^2}{2dn_{\text{eff}}} \quad \text{and} \quad \delta\lambda \sim \frac{\Delta\lambda}{\pi} \frac{1-R}{\sqrt{R}}, \quad (1)$$

respectively, where n_{eff} is the corresponding effective refractive index of the waveguide. Therefore, for $d = 1.5\ \text{mm}$ and $n_{\text{eff}} \sim 4$ (corresponding to $\text{Al}_{0.7}\text{Ga}_{0.3}\text{N}$), the separation of two neighboring modes is expected to be well below 0.01 nm for an emission wavelength shorter than 280 nm, which is below the resolution of our experimental setup. However, if some modes are suppressed a larger spacing will result and the remaining modes can be resolved, as shown in Figures 2(c) and 2(d). However, to unambiguously verify the existence of the longitudinal modes, shorter laser cavities are needed.

Following this observation, significantly shorter cavities were prepared: 180 μm for the MQW and 200 μm for the DH structure. Figure 3 shows the polarization dependent high-resolution lasing spectra for these shorter cavities. The emission peaks of the short cavities were centered at $\sim 281.6\ \text{nm}$ for the MQW and at $\sim 260.5\ \text{nm}$ for the DH structures. Well-defined, equally spaced, *TE* polarized longitudinal modes were clearly observed for both structures. The spacing of the longitudinal modes was 0.059 nm for the MQW and

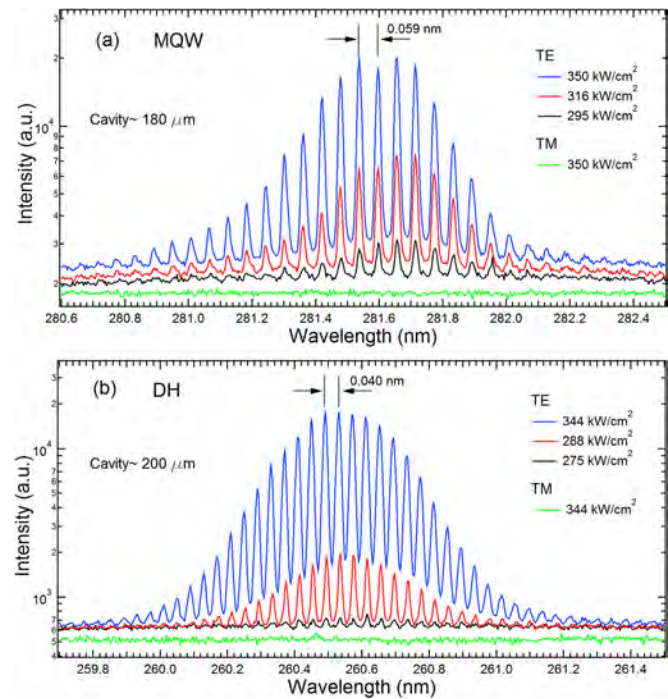


FIG. 3. Polarization-dependent, high-resolution spectra for (a) MQW and (b) DH pumped above the threshold. Longitudinal modes with equal spacing are well resolved. For the 180 μm cavity, the mode spacing was 0.059 nm and a FWHM of each mode was $\sim 0.018\ \text{nm}$. For 200 μm cavity, the mode spacing was 0.040 nm, and a FWHM of each mode was $\sim 0.014\ \text{nm}$. The longitudinal modes were not observed under TM polarization. Spectra are shifted vertically for clarity.

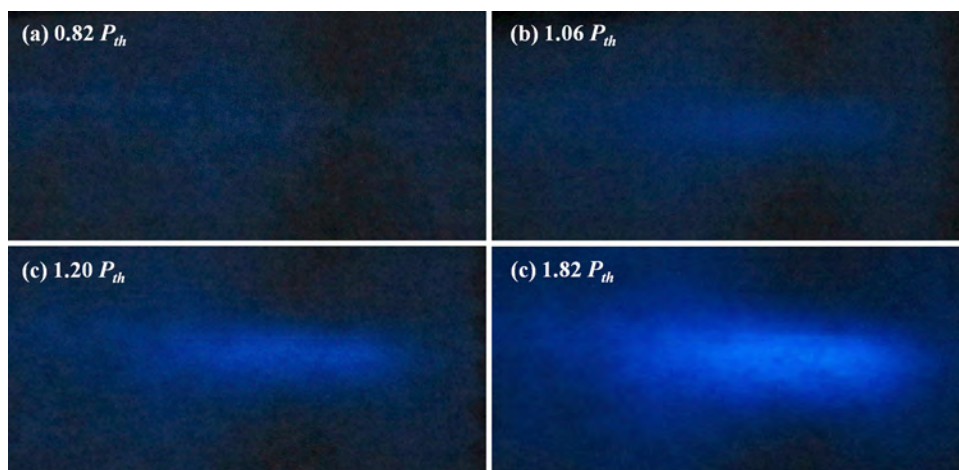


FIG. 4. Far-field patterns for MQW structure pumped below and above the threshold. The laser beam was perpendicular to the screen, which was 1 cm away from the exit facet.

0.040 nm for the DH structure. The FWHM of the individual longitudinal modes was 0.014 nm for the MQW and 0.018 nm for the DH, which correlated well with the expected mode spacing and width calculated from Eqs. (1). Since the mode separation was well above the spectral resolution, changing the integration time did not have any influence on the spectral shape for these short cavities, which is in contrast to the 1.5 mm long cavity. All modes were TE polarized and no transverse magnetic (TM) polarized longitudinal modes were observed. Such polarization-dependent lasing is consistent with theoretical calculations.^{22,23} For all measurements, the emission below threshold was randomly polarized while the lasing peak was always TE polarized, independent of cavity length.

Lasing is highly directional with divergence determined by the cross-section of the cavity; an elliptical far-field pattern is typically observed for an edge-emitting laser due to diffraction on the rectangular exit facet. Far-field patterns are frequently used to verify the achievement of true lasing. Typical far-field patterns for the MQW structure recorded on a screen at different pumping levels are shown in Figure 4. The screen was made of printer paper and was placed ~ 1 cm away from the cavity, with the cavity perpendicular to paper plane. When pumped below the threshold, no clear pattern was observed, as spontaneous emission is emitted randomly in all directions. Above the threshold ($P_{\text{pump}} = 1.06 P_{\text{th}}$), an elliptically shaped pattern appeared on the screen, becoming more intense at higher pumping levels. Noticeable light leakage towards the substrate-side suggests lateral confinement of the light by the 500 nm $\text{Al}_{0.7}\text{Ga}_{0.3}\text{N}$ cladding layer was not ideal.

In summary, we have achieved sub-300 nm lasing in AlGaIn-based MQW and DH structures with thresholds as low as 84 kW/cm^2 . Both structures showed TE polarized emission. Sporadic longitudinal modes were observed for 1.5 mm long cavities; however, the spectral resolution of the spectrometer limited the direct observation of individual longitudinal cavity modes. By reducing the cavity length below $200 \mu\text{m}$, well-resolved, equally spaced longitudinal modes were observed for both structures, indicating deep UV lasing. The FWHM of an individual longitudinal mode was as narrow as 0.014 nm, as expected from cavity parameters. Our results demonstrate that AlGaIn-based sub-300 nm UV lasers

with low threshold can be achieved on single crystal AlN substrates. This achievement serves as a starting point towards realizing electrically pumped sub-300 nm UV lasers.

The authors would like to thank Paul Rozvadovsky of HexaTech for wafer thinning, which made cleaving of short cavities possible.

- ¹S. Nakamura, S. Pearton, and G. Fasol, *The Blue Laser Diode: The Complete Story* (Springer, 2000).
- ²Y. Taniyasu, M. Kasu, and T. Makimoto, *Nature* **441**, 325 (2006).
- ³A. Khan, K. Balakrishnan, and T. Katona, *Nature Photon.* **2**, 77 (2008).
- ⁴H. Yoshida, Y. Yamashita, M. Kuwabara, and H. Kan, *Nature Photon.* **2**, 551 (2008).
- ⁵S. D. Lester, F. A. Ponce, M. G. Craford, and D. A. Steigerwald, *Appl. Phys. Lett.* **66**, 1249 (1995).
- ⁶K. Ban, J.-I. Yamamoto, K. Takeda, K. Ide, M. Iwaya, T. Takeuchi, S. Kamiyama, I. Akasaki, and H. Amano, *Appl. Phys. Express* **4**, 052101 (2011).
- ⁷P. Petroff and R. L. Hartman, *Appl. Phys. Lett.* **23**, 469 (1973).
- ⁸T. Suzuki and Y. Matsumoto, *Appl. Phys. Lett.* **26**, 431 (1975).
- ⁹S. Nakamura, *Science* **281**, 956 (1998).
- ¹⁰V. Adivarahan, W. H. Sun, A. Chitnis, M. Shatalov, S. Wu, H. P. Maruska, and M. A. Khan, *Appl. Phys. Lett.* **85**, 2175 (2004).
- ¹¹D. Ehrentraut and Z. Sitar, *MRS Bull.* **34**, 259 (2009).
- ¹²R. Dalmau, B. Moody, R. Schlessler, S. Mita, M. Feneberg, B. Neuschl, K. Thonke, R. Collazo, A. Rice, J. Tweedie, and Z. Sitar, *J. Electrochem. Soc.* **158**, H530 (2011).
- ¹³M. Feneberg, B. Neuschl, K. Thonke, R. Collazo, A. Rice, Z. Sitar, R. Dalmau, J. Xie, S. Mita, and R. Goldhahn, *Phys. Status Solidi A* **208**, 1520 (2011).
- ¹⁴T. P. Lee, C. Burrus, and B. Miller, *IEEE J. Quantum Electron.* **9**, 820 (1973).
- ¹⁵E. Feltin, A. Castiglia, G. Cosendey, L. Sulmoni, J. F. Carlin, N. Grandjean, M. Rossetti, J. Dorsaz, V. Laino, M. Duellk, and C. Velez, *Appl. Phys. Lett.* **95**, 081107 (2009).
- ¹⁶T. Takano, N. Yoshinobu, H. Akihiko, and K. Hideo, *Appl. Phys. Lett.* **84**, 3567 (2004).
- ¹⁷T. Wunderer, C. L. Chua, Z. Yang, J. E. Northrup, and N. M. Johnson, *Appl. Phys. Express* **4**, 092101 (2011).
- ¹⁸P. E. Francesco, W. Zhang, A. Y. Nikiforov, J. Yin, R. Paiella, L. D. Negro, and T. D. Moustakas, *J. Appl. Phys.* **113**, 013106 (2013).
- ¹⁹A. Rice, R. Collazo, J. Tweedie, R. Dalmau, S. Mita, J. Xie, and Z. Sitar, *J. Appl. Phys.* **108**, 043510 (2010).
- ²⁰D. Stocker, E. F. Schubert, K. S. Boutros, J. S. Flynn, R. P. Vaudo, V. M. Phanse, and J. M. Redwing, *Electron. Lett.* **34**, 373 (1998).
- ²¹S. M. Sze and K. K. Ng, *Physics of Semiconductor Devices* (Wiley-interscience, 2006).
- ²²J. E. Northrup, C. L. Chua, Z. yang, T. Wunderer, M. Kneissl, N. M. Johnson, and T. Kolbe, *Appl. Phys. Lett.* **100**, 021101 (2012).
- ²³J. Zhang, H. Zhao, and N. Tansu, *Appl. Phys. Lett.* **98**, 171111 (2011).